A study on the transport properties in the $Bi_{2-x}Pb_xSr_{1.65}La_{0.35}CuO_y$ system

1997 J. Phys.: Condens. Matter 9 5137

(http://iopscience.iop.org/0953-8984/9/24/012)

J. Phys.: Condens. Matter **9** (1997) 5137–5144. Printed in the UK PII: S0953-8984(97)77403-4

A study on the transport properties in the $Bi_{2-x}Pb_xSr_{1.65}La_{0.35}CuO_y$ system

Xu Gaojie†, Mao Zhiqiang†, Xu Xiaojun†, Tian Mingliang†, Shi Lei† and Zhang Yuheng†‡

† Structure Research Laboratory, University of Science and Technology of China, Hefei, Anhui 230026, People's Republic of China

‡ Chinese Center of Advanced Science and Technology (World Laboratory), PO Box 8730, Beijing, People's Republic of China

Received 27 August 1996, in final form 31 January 1997

Abstract. Samples of the $Bi_{2-x}Pb_xSr_{1.65}La_{0.35}CuO_y$ ($x = 0$, 0.1, 0.2, 0.3, 0.4 and 0.6) system with different oxygen concentration are obtained. The analysis of x-ray diffraction indicates that a tetragonal–orthorhombic transition takes place with increase of Pb content. The resistivity measurement shows that for the quenched samples the highest T_c^{onset} is 35 K, and T_c^0 (zero resistivity) is 25 K; while for the samples annealed under low oxygen partial pressure, the highest T_c^{onset} and T_c^0 increase to 45 K and 37 K, respectively. Moreover, the phenomenon of a spin gap is systematically observed in this system. The analysis of the experimental results reveals that the microstructural characteristic of the Bi2201 system is closely related to both the spin-paring and superconductivity. The dominated spin scattering mechanism is suggested as the origin of the T-linear resistivity.

1. Introduction

It is generally realized that the physical properties of the CuO_2-based superconducting systems are strongly related to the carrier concentration. For example, in the $YBa_2Cu_3O_y$ system [1], T_c can be increased from 60 to 90 K by changing oxygen concentration. For a polycrystalline $Bi_2Sr_2CaCu_2O_y$ system [2–4], T_c can be improved from 65 to 92 K by the removal of a small amount of oxygen. However, sometimes we cannot obtain the highest T_c by only regulating the oxygen content. For example, the oxygen content in the Bi2201 system is not the only factor in determining T_c, and the structural factor also plays an important role in influencing the superconductivity [5–7].

In order to understand the relationship between the structure and normal-state properties of cuprate superconductors, many theoretical and experimental studies have focused on the Bi2201 system [5, 8–15]. This is because the Bi2201 system not only possesses a complicated incommensurate modulation structure, but also exhibits a much wider temperature region where the normal-state exists, which allows one to measure the normal-state transport properties to lower temperature than in other high-T_c materials. Among the elemental-doped $Bi_2Sr_2CuO_y$ systems, La doping is more effective in increasing T_c [5, 16]. However, it is known that, although La doping can increase T_c, it enhances the structural distortion [17]. If the distortion of the La-doped Bi2201 phase is relaxed, further improvement of superconductivity is possible, because strongly structural distortion can suppress the superconducting transition. In this paper, we perform Pb doping to

0953-8984/97/245137+08$19.50

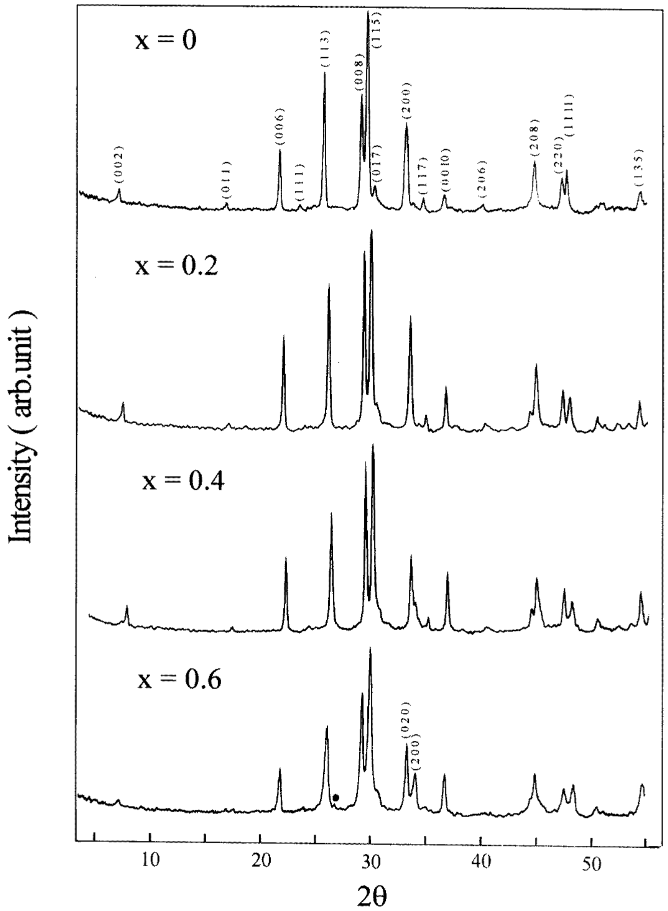

Figure 1. The powder x-ray diffractions for samples of the $Bi_{2-x}Pb_xSr_{1.65}La_{0.35}CuO_y$ system (x = 0, 0.2, 0.4, 0.6); the peaks marked with a full circle (●) correspond to the reflections of the impurity phases.

relax the structural distortion of the $Bi_2Sr_{2-x}La_xCuO_y$ system, and make a systematical investigation of the normal-state transport properties, as well as the relation of the structure and superconductivity.

2. Experimental details

Samples were prepared by the conventional solid-state reaction method. Appropriate high-purity powders of Bi_2O_3, La_2O_3, $SrCO_3$ and CuO were mixed with a nominal composition of $Bi_{2-x}Pb_xSr_{1.65}La_{0.35}CuO_y$ (x = 0, 0.1, 0.2, 0.3, 0.4 and 0.6), then preheated in air at 820 °C for 24 h. In order to ensure the complete reaction of the reactant oxides, the products were reground and reheated in air at 830 °C for another day. Then the powders were pressed into pellets, sintered in air in the temperature range 840–860 °C for 2 days, and finally quenched in air. (This series of samples is denoted as A_1, B_1, C_1, D_1, E_1 and F_1 for $x = 0$, 0.1, 0.2, 0.3, 0.4 and 0.6, respectively.) Some of the quenched samples were

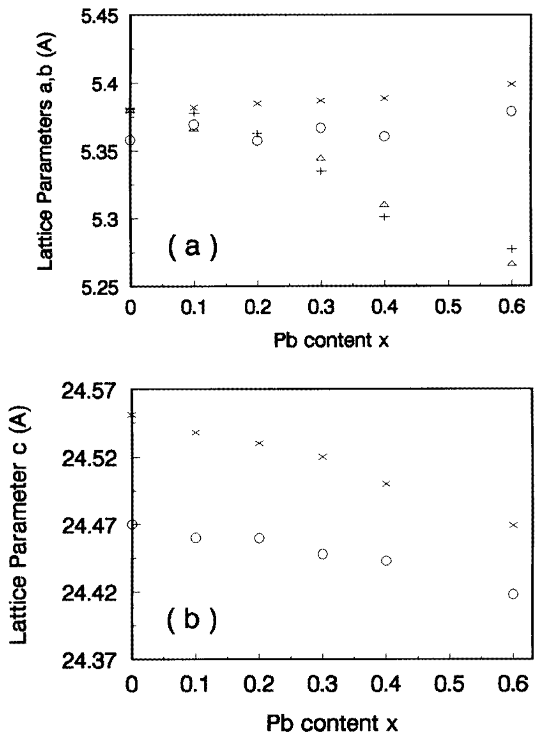

Figure 2. (a) Variation of lattice parameters a and b with Pb content x in the $Bi_{2-x}Pb_xSr_{1.65}La_{0.35}CuO_y$ system. For the quenched samples: $\times, a$; $+, b$. For the samples annealed under an O_2 pressure of 10^{-5} atm: ○, a; △, b. (b) Variation of lattice parameter c with Pb content x in the $Bi_{2-x}Pb_xSr_{1.65}La_{0.35}CuO_y$ system. ○, the quenched samples, $\times$, for the samples annealed under an O_2 pressure of 10^{-5} atm.

further annealed at 550 °C under an oxygen partial pressure of 10^{-5} atm for 3 h, and these samples are denoted correspondingly as A_2, B_2, C_2, D_2, E_2 and F_2.

X-ray diffraction (XRD) analysis was carried out on a Rigaku-D/max-γA diffractometer using high-intensity Cu-Kα radiation. The lattice parameters were determined from the d-values of XRD peaks by a standard least-squares refinement method. Resistivity for all the samples was measured using a standard four-probe method in a closed-cycle helium cryostat.

3. Results and discussion

The XRD analysis shows that all the prepared samples remain single phase except the samples F_1 and F_2, and annealing under an oxygen partial pressure of 10^{-5} atm does not cause phase decomposition. Figure 1 displays the typical XRD patterns for the quenched samples A_1, C_1, E_1 and F_1. The impurity phase peaks are denoted by solid circle. The lattice parameters a, b and c are shown in figure 2(a) and (b). Following figure 2 it can be seen that the parameters b and c decrease continuously as Pb content increases, while a increases. The change of the lattice parameters clearly indicates that a tetragonal–orthorhombic transition takes place with the increase of Pb content, which is consistent with the split of (0 2 0) and (2 0 0) peaks (see figure 1). On the other hand, the annealing treatment under low oxygen

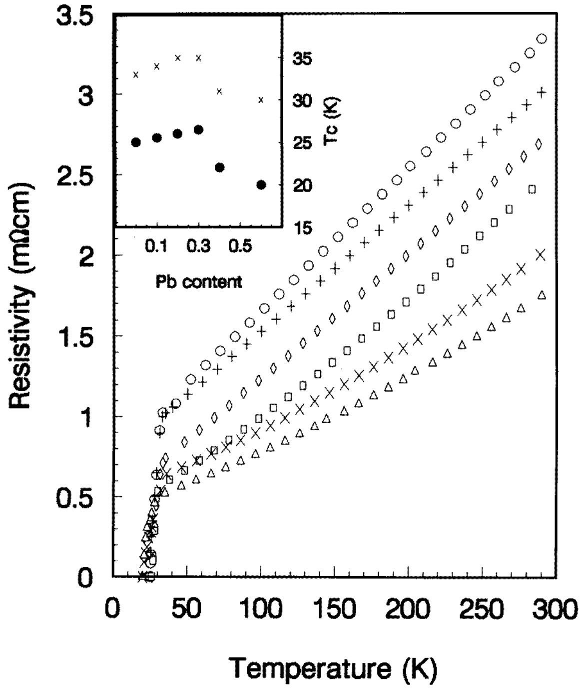

Figure 3. Temperature dependence of the resistivity for the quenched samples of the $Bi_{2-x}Pb_xSr_{1.65}La_{0.35}CuO_y$ system (○, $x = 0$; +, $x = 0.1$; ◊, $x = 0.2$; □, $x = 0.3$; △; $x = 0.4$; ×, $x = 0.6$). The inset shows T_c^{onset} (×) and T_c^0 (●) as a function of Pb content x.

partial pressure produces lattice parameters which are greater than those observed with the corresponding quenched samples.

Figure 3 shows the temperature-dependent resistivity for samples A_1, B_1, C_1, D_1, E_1 and F_1. All the samples show a superconducting transition. T_c^{onset} and T_c^0 (zero resistivity) for these samples are shown in the inset. From the T_c values, one can see that appropriate Pb substitution for Bi in the $Bi_{2-x}Sr_{1.65}La_{0.35}CuO_y$ system can increase T_c^{onset} and T_c^0, while heavy Pb doping results in decreasing T_c. Samples A_1, B_1 and C_1 exhibit a T-linear resistivity above T_c, while samples D_1, E_1 and F_1 show a faster than linear increase in resistivity as shown in figure 3. Obviously, the samples D_1, E_1 and F_1 lie in the overdoped region. We plot the resistivity for samples D_1, E_1 and F_1 as $\ln(\rho - \rho_0)$ versus $\ln(T)$ in figure 4. It can be seen that the resistivity approximately follows a simple power law $\rho - \rho_0 = \alpha T^n$. The best linear fit of the data gives $n = 1.11$, 1.25 and 1.23, and $\rho_0 = 0.4$, 0.41 and 0.52 mΩ for samples D_1, E_1 and F_1, respectively. A similar behaviour is also found in other overdoped systems, for example, in $La_{2-x}Sr_xCuO_4$ [18] an exponent $n \sim 2$ is obtained for the overdoped sample with $x = 0.3$; in the $Tl_2Ba_2CuO_y$ system [19], the exponent n changes gradually from 1 to 2 with the samples changing from superconductor to an overdoped normal metal.

Figure 5(a) shows the temperature-dependent resistivity for samples A_2, B_2, C_2, D_2, E_2 and F_2. All the samples still show a superconducting transition. T_c^{onset} and T_c^0 are shown in figure 5(b). By comparison with the inset of figure 3, it can be seen that the annealing treatment improves the superconductivity remarkably. The highest T_c^{onset} increases from 35 to 45 K and T_c^0 increases from 25 to 37 K. This result not only indicates that the carrier

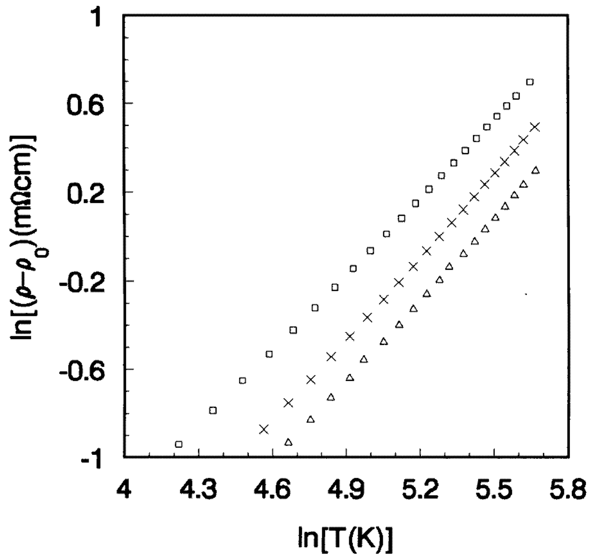

Figure 4. $\ln(\rho - \rho_0)$ as a function of $\ln(T)$ for samples D_1 (□), E_1 (△) and F_1 (×). The best fit gives $n = 1.11$, 1.25 and 1.23, respectively.

concentration is closely related to the superconductivity, but also reveals that the crystal microstructure has a strong influence on the superconducting transition. It is known that Pb doping of $Bi_2Sr_2CuO_y$ can lower the monoclinic modulation [17]; when the dopant (Pb) concentration $x \geqslant 0.2$, the monoclinic modulation disappears and merely the orthorhombic modulation induced by Pb doping exists. With further increase of Pb content, all the modulation disappears. For our samples, Pb doping relaxes the structural distortion, hence improving the superconductivity. This result is in agreement with the suggestion of Onoda and Sato [20] and Gao *et al* [21] that the deviation of the Cu-atom positions from the *a–c* plane caused by the modulation wave in the 2201 phase may be one of the origins of the rather low T_c value of the Bi–Sr–Cu–O compound, and also supports the view of Mao *et al* [6] that the crystal microstructure has a direct relation with high-T_c superconductivity. Now let us look at the shape of the curves in figure 5. Sample A_2 shows a semiconductor-like behaviour above T_c. For sample B_2, the $\rho(T)$–T curve exhibits an unusual phenomenon, i.e. above 170 K the $\rho(T)$ shows a semiconductor-like behaviour, while below 170 K the conduction shows a metal-like behaviour. For samples C_2, D_2, E_2 and F_2, the resistivity in the normal state is not exactly linearly temperature dependent, a downturn in the $\rho(T)$–T curves can be seen around 170 K which is closely related to the opening of a spin gap, as will be discussed elsewhere [22]. In order to clearly observe the deviation of the resistivity from T-linearity, we replot the data for samples C_2, C_2, D_2 and E_2 as $[\rho(T) - \rho(0)]/\alpha T$ versus T in figure 6, where α is the slope of the T-linear region of the $\rho(T)$–T curve and $\rho(0)$ is the extrapolated value to $T = 0$ K from the T-linear region. From figure 6, we can see that the temperature (T^*), where the resistivity begins to deviate downward from T-linearity, increases gradually from sample E_2 to D_2 to C_2, which is coincident with the decrease of carrier concentration. In other words, the spin-gap temperature increases gradually with decreasing carrier concentration.

It is commonly believed that a spin gap usually occurs in the underdoped region of the phase diagram. Yet, for the $Bi_2Sr_{2-x}La_xCuO_y$ system, we cannot observe the spin gap in

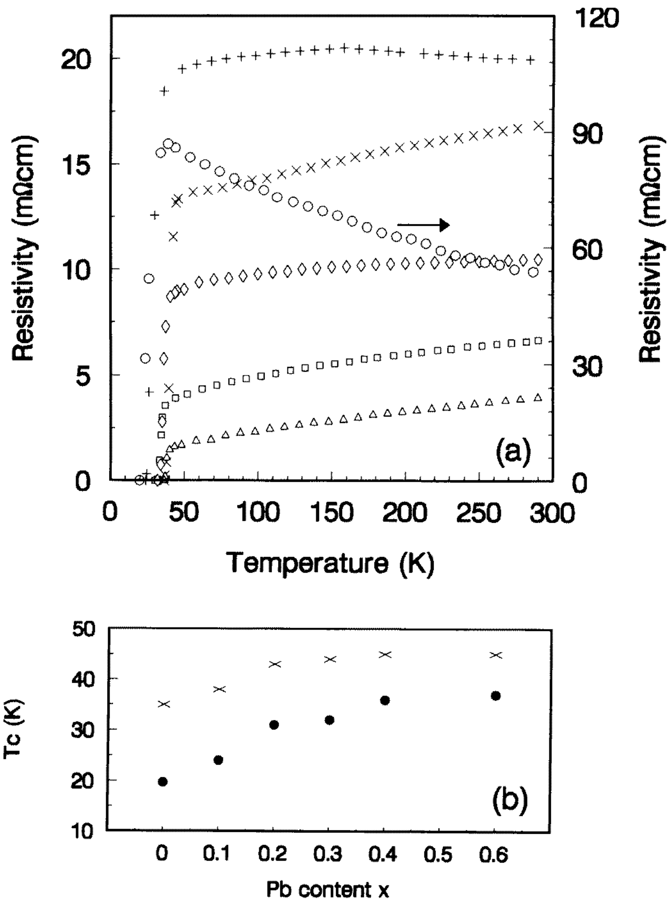

Figure 5. (a) The temperature-dependent resistivity for samples $Bi_{2-x}Pb_xSr_{1.65}La_{0.35}CuO_y$ (○, $x = 0$; +, $x = 0.1$; ◊, $x = 0.2$; □, $x = 0.3$; △, $x = 0.4$; ×, $x = 0.6$) annealed under an O_2 pressure of 10^{-5} atm. (b) T_c^{onset} (×) and T_c^0 (●) as a function of Pb content x for samples $Bi_{2-x}Pb_xSr_{1.65}La_{0.35}CuO_y$ annealed under an O_2 pressure of 10^{-5} atm.

the underdoped region. This is not to say that the spin gap does not exist in the Bi2201 phase. In fact, a spin gap does exist in the underdoped region of the Bi2201 system with a proper microstructure. Here, the microstructural characteristic plays an important role in determining the spin excitation spectrum. The strongly structural distortion changes the orientation of Cu^{2+} spins and influences the interplay of these spins, thus impeding the effective spin-paring and suppressing the occurrence of a spin gap.

Due to the spin gap not being found in the Bi2201 system for a long time, there are few reports to discuss the normal-state transport properties in terms of spin scattering. It is known that among the unusual normal-state properties, the observed linear temperature dependence of the electrical resistivity extending from the critical temperature T_c up to very high temperature remains a puzzling question [19, 22–25]. Martin *et al* [10] fitted their resistivity data to the Bloch–Grüneisen formula and found an unphysically low transport Debye temperature of less than 35 K. Hou *et al* [25] pointed out that the electron–phonon mechanism was inadequate to account for the electrical transport along the *a*–*b* plane in

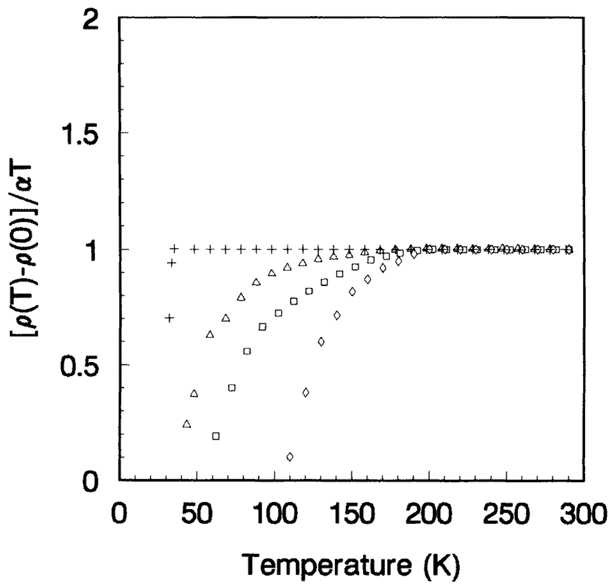

Figure 6. $[\rho(T) - \rho(0)]/\alpha T$ as a function of temperature (+, C_1, ◊; C_2; □, D_2; △, E_2) where $\rho(0)$ is the $T = 0$ intercept of the line extrapolated from the T-linear part and α is the slope of the T-linear resistivity.

the cuprates. Ando *et al* [26] reported that the in-plane resistivity in the La-doped Bi2201 system exhibited a T-linear behaviour down to 0.66 K. However, Vedeneer *et al* [27] argued that the in-plane resistivity of the Bi2201 phase could be described well by Bloch–Grüneisen theory. Up to now, no consensus has been achieved on the T-linear resistivity in the Bi2201 system. Our experimental result of the strong dependence of T^* on oxygen concentration rules out the possibility of phonon scattering. The scattering by spin fluctuation should be the most plausible candidate as the origin of T-linear resistivity. From figure 5(a), one can see that, above the spin-gap temperature, samples C_2, D_2, E_2 and F_2 all exhibit a T-linear resistivity, where $\rho \propto T$, and when the spin gap opens the spin scattering decreases, thus producing a turndown in the ρ–T curve. Obviously, the spin scattering in the normal-state transport plays a critical role. If no spin gap occurred, the T-linear resistivity would exist down to a very low temperature. In fact, when some strongly structural distortion exists in the Bi2201 system, there is no spin gap occurring. For example, in the $Bi_{2.1}Sr_{1.9-x}La_xCuO_y$ system, we did not observe the features associated with the spin gap either in resistivity or in thermoelectric power. Pb doping of the Bi2201 system can lower the structural distortion, as has been discussed above, so we can easily observe the spin-gap phenomenon in this system. All the above analysis demonstrates that the microstructural characteristic, along with the carrier concentration, determines the spin excitation spectrum. Moreover, in spite of whether the spin gap exists or not, the spin scattering always exists and the spin scattering mechanism is still the origin of the T-linear resistivity.

In summary, we have successfully obtained samples of the $Bi_{2-x}Pb_xSr_{1.65}La_{0.35}CuO_y$ system with different carrier concentrations. The XRD analysis indicates that a tetragonal–orthorhombic transition takes place with increase of Pb content. The improvement of T_c reveals that the crystal microstructure has a significant influence on the superconductivity. Additionally, the spin scattering mechanism is also suggested as the origin of the T-linear resistivity in the Bi2201 system.

References

[1] Shin-ichi Uchida 1993 *Japan. J. Appl. Phys.* **32** 3784
[2] Triscone G, Genoud J Y, Graf T, Junod A and Muller J 1990 *Physica* C **176** 247
[3] Nagoshi M, Suzuki T, Fukuda Y, Terashima K, Nakanishi Y, Ogita M, Tokiwa A, Syono Y and Tachiki M 1991 *Phys. Rev.* B **43** 10 445
[4] Sieburger R, Muller P and Schilling J S 1991 *Physica* C **181** 335
[5] Maeda A, Hase M, Tsukada I, Noda K, Takebayashi S and Uchinokura K 1990 *Phys. Rev.* B **41** 6418
[6] Mao Zhiqiang, Tian Mingliang, Wang Ruiping and Zhang Yuheng 1994 *Phys. Rev.* B **49** 9857
[7] Groen W A, De leenw D M and Stollman G M 1989 *Solid State Commun.* **72** 697
[8] Tarascon J M, Mckinnon W R, BarBoux P, Hwang D M, Bagley D G, Greene L H, Hull G W, Le Page Y, Stoffel N and Giroud M 1988 *Phys. Rev.* B **38** 8885
[9] Xiao G, Ciplak M Z and Chien C L 1988 *Phys. Rev.* B **38** 11 824
[10] Martin S, Fiory A T, Fleming R M, Schneemeyer L F and Waszczak J V 1990 *Phys. Rev.* B **41** 846
[11] Vedeneev S I, Jansen A G M, Tsvetkov A A and Wyder P *Phys. Rev.* B **51** 16 380
[12] Mao Zhiqiang, Zhang Hongguang, Tian Mingliang and Zhang Yuheng 1993 *Phys. Rev.* B **48** 16 135
[13] Matsui Y, Maeda M, Uchinokura K and Takekawa S 1988 *Japan. J. Appl. Phys.* **27** L1873
[14] Sera M, Tanaka S, Sato M and Fujishita H 1992 *Solid State Commun.* **81** 415
[15] Bauhofer W, Mattausch H, Kremer R K, Murugaraj P and Simon A 1989 *Phys. Rev.* B **38** 7244
[16] Xu Gaojie, Mao Zhiqiamg, Tian Mingliang and Zhang Yuheng, submitted
[17] Mao Zhiqiang, Fan Chenggao, Shi Lei and Zhang Yuheng 1993 *Phys. Rev.* B **47** 14 467
[18] Kubo Y, Sera M, Yamagata S, Kondoh S, Onoda M and Sato 1989 *Solid State Commun.* **70** 303
[19] Kubo Y, Shimakawa Y, Manako T and Igarashi H 1991 *Phys. Rev.* B **43** 7875
[20] Onoda M and Sato M 1988 *Solid State Commun.* **67** 799
[21] Gao Y, Lee P, Ye J, Bush P, Petricek V and Coppens P 1989 *Physica* C **160** 431
[22] Xu Gaojie, Mao Zhiqiang, Wang Ruiping and Zhang Yuheng, unpublished
[23] Gurvitch M and Fiory A T 1987 *Phys. Rev. Lett.* **59** 1337
[24] Takagi H, Batlogg B, KaoJ. Kwo H L, Cava R J, Krajewski J J and Peck W P 1992 *Phys. Rev. Lett.* **69** 2975
[25] Hou X H, Zhu W J, Li J W, Xiong W, Wu F, Huang Y Z and Zhao Z X 1994 *Phys. Rev.* B **50** 496
[26] Ando Y, Boebinger G S, Passner A, Wang N L, Geibel C and Steglich F *Phys. Rev. Lett.* submitted
[27] Vedeneev S L, Jansen A G M, Tsvetkov A A and Wyder P 1995 *Phys. Rev.* B **51** 16 380